SCREEN-PRINTED BACK SURFACE REFLECTOR FOR LIGHT TRAPPING IN CRYSTALLINE SILICON SOLAR CELLS

A. Ristow, M. Hilali, A. Ebong, A. Rohatgi
School of Electrical and Computer Engineering, Georgia Institute of Technology
Atlanta, Georgia 30332-0250 USA

ABSTRACT: Evaporated metal back surface reflectors have been shown to yield high values of internal rear reflectance, and are particularly effective when combined with a thin dielectric layer between the silicon and the metal. However, evaporated metals are not compatible with low-cost solar cell fabrication processes and generally do not scatter light well, resulting in inefficient trapping of light. In this work, affordable screen-printed metal pastes have been employed to fabricate effective low-cost back surface reflectors. The best of these, fabricated from screen-printed silver paste on a thin silicon nitride dielectric layer, yield back surface reflectance values similar to those of evaporated metal reflectors. Furthermore, the screen-printed back surface reflectors in this study are shown to be highly diffuse, thus enhancing light trapping in planar silicon solar cells. PC1D simulations suggest that a solar cell with a screen-printed metal/dielectric back surface reflector should outperform one with a high-quality aluminum back surface field.
Keywords: Light Trapping — 1: Passivation — 2: Screen Printing — 3

1. INTRODUCTION

Metal and metal/dielectric back surface reflectors (BSRs) can yield internal reflectance values greater than 90% [1]. These reflectors typically consist of a thick thermal oxide and evaporated metal layer, and enhance surface passivation as well as light trapping. However, evaporated metals are generally regarded as too costly for application to commercial terrestrial-grade solar cells. Furthermore, these reflectors tend to be highly specular, limiting prospects for light trapping in solar cells with planar surfaces.

It has been shown that a randomizing, or Lambertian, BSR provides a very high degree of light trapping for solar cells with planar front surfaces by restricting escape reflectance via total internal reflection at the front surface [2]. In such a scheme, radiation incident upon the rear interface is randomly scattered in a direction independent of the angle of incidence. Light scattered from the back surface and incident upon the front may only be coupled out of the solar cell for angles of incidence less than the critical angle, ϕ_c, measured from normal. The range of angles from 0 to ϕ_c fills a conical volume called the *loss cone*. Light incident upon the internal front surface at angles greater than ϕ_c is totally internally reflected, while the remainder may be coupled out of the cell. The value of ϕ_c is equal to $\sin^{-1}(1/n)$, where n is the index of refraction of the substrate [3]. Further analysis reveals that for an ideal Lambertian reflector the amount of reflected light lost through the front surface is equal to $\sin^2 \phi_c = 1/n^2$ [2]; for silicon at 1200 nm, $n = 3.52$ and the loss through the front surface is 8%. Antireflection coatings do not affect this result.

It is important to understand the impact of small changes in back surface reflectance in a Lambertian light trapping scheme. Assuming insignificant optical absorption in the bulk, a ray of light will persist via multiple internal reflections until it is either absorbed by the BSR or escapes through the front surface of the solar cell. Given that only 8% of the light will escape through the front surface on each pass through the cell, a ray may be reflected many times before escaping. If the back surface reflectance, R_b, is 95%, about 14% of the light will be absorbed in the reflector after three passes through the cell ($1 - 0.95^3$). If R_b is 90%, about 27% of the light will be absorbed after three passes. If R_b is 80%, absorption in the BSR will be about 49% after three passes. Thus, very small changes in R_b can have a very large effect on the observed escape reflectance.

A similar analysis of internal front surface reflectance may be carried out for specular BSRs. Considering for simplicity only light normally incident upon the solar cell, the reflectance R at an interface coated with a single-layer antireflection coating may be expressed as [3]

$$R = \frac{n_1^2(n_0 - n_s)^2 \cos^2 \delta + (n_0 n_s - n_1^2)^2 \sin^2 \delta}{n_1^2(n_0 + n_s)^2 \cos^2 \delta + (n_0 n_s + n_1^2)^2 \sin^2 \delta}, \qquad (1)$$

where n_0, n_1, and n_s are the indices of refraction for air, the antireflection coating, and the substrate, respectively; and the phase difference $\delta = (2\pi/\lambda)n_1 t$, where λ is the wavelength of the incident light and t is the thickness of the antireflection coating. Note that the values of n_0 and n_s may be reversed in equation (1) without affecting the result; that is, the reflectance is the same regardless of the direction of the wave.

Front surface reflectance at 1200 nm is typically around 20% for a single-layer antireflection coating, suggesting that 80% of the light reflected from a specular BSR will escape through the front surface. Thus a cell with a perfectly Lambertian BSR will lose just 8% of the light reflected from the rear surface on each pass, while one with a perfectly specular BSR will lose ten times as much. Therefore, the advantage of a Lambertian BSR for light trapping is obvious.

This work demonstrates a commercially viable method of using screen-printed metal pastes to produce highly Lambertian BSRs with internal reflectance values approaching that of conventional specular evaporated reflectors. Metal/dielectric reflectors are fabricated using silicon nitride (SiN_x) deposited by plasma-enhanced chemical vapor deposition (PECVD), which possesses excellent passivation properties [4] and is resistant to etching by fritless metal pastes. Experimental evidence of the feasibility and Lambertian character of such reflectors, as well as the specular nature of evaporated reflectors, is supplemented by PC1D modeling of hypothetical devices incorporating these reflectors as design features. It is shown that, when surface passivation effects are taken into account, a screen-printed Ag/dielectric BSR can outperform both a high-quality Al back surface field (BSF) and an evaporated Ag/dielectric BSR.

2. EXPERIMENTAL METHOD

2.1. Sample Preparation

Reflectors were fabricated on 100 μm-thick silicon substrates grown by the dendritic web technique. The front surface of each sample was coated with a single-layer SiN_x antireflection coating 780 Å thick, with an index of refraction of 1.99 at 632.8 nm. Samples with metal/dielectric BSRs also received the same coating on the rear surface. Metallization was applied by screen-printing one of two metal pastes onto the rear surface and firing in a belt furnace for 2 min at setpoint temperatures of 300–850°C.

The two metal pastes included an Al paste, Ferro FX53-038, containing glass frit intended to etch residual surface coatings and the silicon surface itself. Fritted pastes generally etch SiN_x at high processing temperatures. The second paste was a fritless Ag paste, DuPont PV167, which does not etch the SiN_x dielectric. In this manner, the samples were divided into four categories: (1) Ag metal reflector, (2) Ag metal/dielectric reflector, (3) Al metal reflector, (4) Al metal/dielectric reflector.

As controls, metal and metal/dielectric reflectors were also fabricated using evaporated Ag and Al.

2.2. Reflector Characterization

Total hemispherical reflectance for each sample was measured using an Optronic Laboratories OL 750 spectroradiometric measurement system with an integrating sphere. The integrating sphere captures all light reflected from the surface of the sample, as well as that escaping from the interior of the sample. In this manner, light scattered by the BSR may be collected and measured. Specular reflectance was also measured for the purpose of estimating what fraction of the total reflectance represents scattered light.

3. RESULTS AND DISCUSSION

3.1. Data Analysis

The fraction of light, β, scattered by the BSR can be estimated by [5]

$$\beta = 1 - \frac{R_{dir} - R_{fe}}{(R_{dir} - R_{fe})R_{fe} + (1 - R_{fe})^2}, \qquad (2)$$

where R_{dir} is the measured specular component of the reflectance, which includes contributions from both the front surface and the BSR, and R_{fe} is the external reflectance of the front surface. Thus, if $R_{dir} \approx R_{fe}$ then $\beta \approx 1$ and all light incident upon the back surface is scattered.

The value of R_{fe} is estimated by linearly extrapolating the surface reflectance between 700–910 nm to 1200 nm. This method tends to overestimate R_{fe}, which can artificially inflate the value of β produced by equation (2). Table I compares the measured specular reflectance values R_{dir} with the estimated values of R_{fe} for screen-printed samples processed at 600°C, as well as for evaporated samples. The near-unity β values suggest that these screen-printed BSRs are nearly perfect Lambertian reflectors. However, due to overestimation of R_{fe}, the true β values are, in reality, somewhat lower than those reported in Table I.

To place a lower bound on the value of β, consider a solar cell with a perfect antireflection coating ($R_{fe} = 0\%$). Equation (2) then becomes $\beta = 1 - R_{dir}$. Thus, the lower limit on the values of β shown in Table I is roughly 0.80. The highest values observed for R_{dir} were ~ 35% for metal-only reflectors processed at low temperatures (300–400°C); however, R_{dir} values for most of the screen-printed reflectors in this study were in the range of 20–25%. Therefore, a lower bound of 0.75–0.80 may be placed on β for the majority of theses screen-printed reflectors. Furthermore, the low-temperature screen-printed metal-only reflectors have β no less than 0.65.

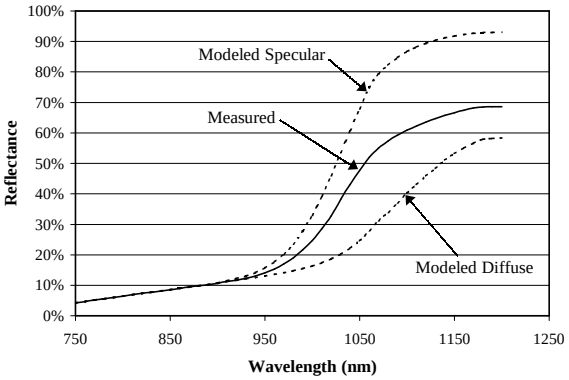

Figure 1: Measured and modeled total reflectance curves for screen-printed Al metal/dielectric BSR processed at 600°C.

That the true value of β is somewhat less than unity is supported by the measured and modeled reflectance curves in Figure 1. The solid curve shows the measured total reflectance for a screen-printed Al metal/dielectric BSR processed at 600°C. The dashed curves show the results of PC1D modeling. The upper dashed curve assumes a perfectly specular BSR with R_{fi} equal to R_{fe} at 1200 nm. The lower dashed curve assumes a perfectly diffuse BSR (R_{fi} = 92%). The analysis to follow estimates R_b at 95% for this sample, and this value was used in the PC1D simulations. Since the measured curve lies between the two modeled curves, the BSR must have some degree of specular character. Thus, the screen-printed reflectors in this study are highly diffuse, but not perfectly so.

Note also from Table I that $R_{dir} \gg R_{fe}$ for the evaporated reflectors, yielding relatively low values of β. Therefore, these reflectors are highly specular.

Reflectance and scattering at the back surface are relevant only for the long-wavelength light that will reach the back of the solar cell. Furthermore, because these wavelengths are weakly absorbed in silicon [1], rays that do not escape through the front surface of the cell will undergo multiple internal reflections. If a large fraction of the light reaching the BSR is scattered, the distribution of photons within

Table I: Comparison of measured specular reflectance (R_{dir}) to estimated surface reflectance (R_{fe}) at 1200 nm and the corresponding value of the β parameter. Values shown for screen-printed (SP) reflectors are from samples processed at 600°C.

Reflector	R_{dir}	R_{fe}	β
SP Al metal	23.0%	21.0%	0.97
SP Al metal/dielectric	24.0%	23.7%	0.99
SP Ag metal	19.1%	17.5%	0.98
SP Ag metal/dielectric	22.4%	21.0%	0.98
Evap. Al metal	72.7%	23.9%	0.30
Evap. Al metal/dielectric	77.5%	24.2%	0.24
Evap. Ag metal	76.5%	26.8%	0.26
Evap. Ag metal/dielectric	84.8%	25.1%	0.16

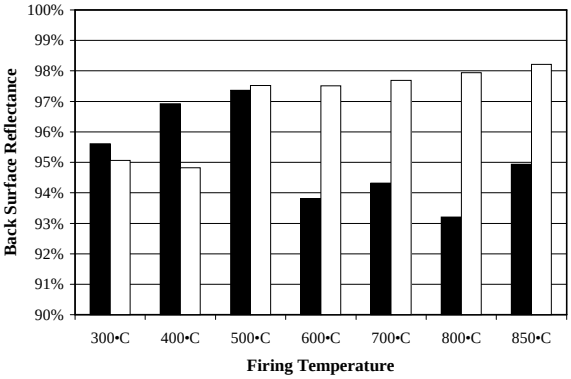

Figure 2: Back surface reflectance for screen-printed Ag reflectors. ■ denotes metal reflectors and □ denotes metal/dielectric reflectors.

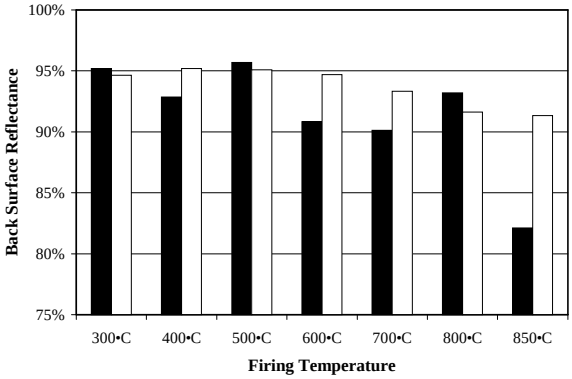

Figure 3: Back surface reflectance for screen-printed Al reflectors. ■ denotes metal reflectors and □ denotes metal/dielectric reflectors.

the cell should be indistinguishable from that of a solar cell with perfectly Lambertian surfaces (i.e., both transmitted and reflected photons scattered randomly upon encountering a surface). This condition has been investigated previously by Gee [6]. Since the screen-printed reflectors exhibit a high level of scattering, we have used Gee's analysis to determine the upper bound of the internal back surface reflectance, R_b.

According to [6], for long-wavelength light and a highly-diffuse BSR, total hemispherical reflectance R_T may be expressed as

$$R_T = R_{fe} + \frac{(1 - R_{fe})(1 - R_{fi})T^2 R_b}{1 - T^2 R_b R_{fi}}, \tag{3}$$

where R_{fe} and R_{fi} are the external and internal values of the front surface reflectance, respectively, R_b is the internal back surface reflectance, and T is the transmittance through the bulk. At long wavelengths, silicon absorbs weakly enough that T may be assumed equal to unity. Solving equation (3) for R_b yields

$$R_b = \frac{R_T - R_{fe}}{(1 - R_{fe})(1 - R_{fi}) + (R_T - R_{fe})R_{fi}}. \tag{4}$$

Recall that when the BSR is Lambertian, $R_{fi} = 92\%$. R_T is known from hemispherical reflectance measurement, and R_{fe} is estimated as detailed previously. For the screen-printed reflectors considered in this work, $R_T \gg R_{fe}$ so that equation (4) is relatively insensitive to errors in the value of R_{fe}. Thus, equation (4) may be used to estimate R_b.

For specular ($\beta \approx 0$) BSRs, such those produced from the evaporated metals, equation (1) shows that $R_{fe} = R_{fi}$. Since R_{fe} is low for a surface bearing an antireflection coating, it follows that light reflected from a specular BSR is likely to escape from the solar cell or be absorbed in the reflector with few internal reflections. Therefore, $R_b \approx R_T$ at 1200 nm provides a reasonable approximation for the specular BSRs in this study [7]. The results are shown in Table II.

3.2. Evaluation of Screen-Printed Reflectors

Values of R_b obtained from equation (4) for the screen-printed Ag reflectors are shown in Figure 2. The screen-printed Ag metal reflector has R_b values in excess of 95% at low processing temperatures, but suffers slightly at temperatures of 600°C and above. This is presumably an effect of the Ag paste reacting with silicon at high temperature. The screen-printed Ag metal/dielectric reflector improves with increasing temperature, yielding an R_b value in excess of 98% at 850°C. This value is similar to that of the evaporated Ag reflectors.

Figure 3 shows the variation of R_b with processing temperature for the Al screen-printed reflector. At low temperatures the metal reflector is similar to the metal/dielectric reflector, with R_b values approaching 95%. However, at temperatures of 600°C and higher the Al begins to alloy with the silicon and reduce R_b. At a processing temperature of 850°C, the metal reflector has an R_b of just 82%. Note that this case corresponds to a typical screen-printed Al BSF.

The Al metal/dielectric reflector, while giving better results than the metal-only reflector, also shows degradation in R_b at high processing temperatures. This is thought to result from the glass frit present in the paste etching the SiN_x dielectric layer. However, R_b values for the Al metal/dielectric reflector remain higher than for the metal-only reflector, particularly at 850°C. This may indicate that the SiN_x layer etches slowly and prevents the Al paste from reaching the silicon at the back surface.

3.3. Modeling the Effect on Device Efficiency

The effect of R_b on device efficiency was modeled in PC1D. The simulated devices were planar and assumed to be 100 μm thick, with bulk resistivity of 1 Ω·cm, bulk lifetime of 20 μs, and sheet resistivity of 40 Ω/□. Series resistance was set 1 Ω·cm^2, shunt resistance to 500 Ω, and a shunt diode with a saturation current density of 10 nA/cm^2 and ideality factor of 2 was also added. Front surface recombination velocity was set to 220,000 cm/s. A measured reflectance curve was used for external front reflectance, and internal front reflectance was set to 92%, consistent with the result from [2] cited in the introduction.

Back surface recombination velocity (S_b) was set differently for the two reflector types. For metal-only reflectors, an ohmic contact was assumed and S_b was set to 10^6 cm/s.

Table II: Back surface reflectance for evaporated reflectors.

Reflector	R_b
Al metal	86.3%
Al/dielectric	92.2%
Ag metal	95.8%
Ag/dielectric	97.0%

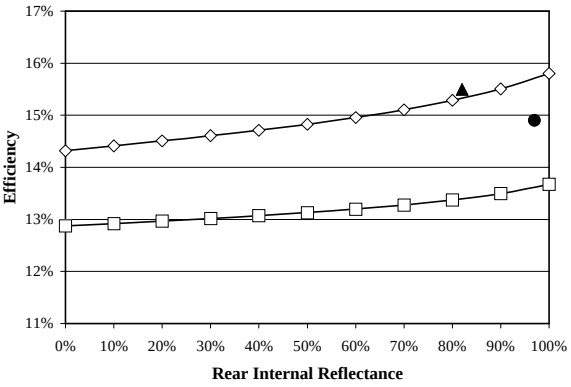

Figure 4: Efficiency as a function of back surface reflectance for screen-printed metal ($S_b = 10^6$ cm/s, denoted by □) and metal/dielectric ($S_b = 1250$ cm/s, denoted by ◊) BSRs. Solar cell efficiencies with a screen-printed BSF and an evaporated Ag metal/dielectric reflector are denoted by ▲ and •, respectively.

For metal/dielectric reflectors, S_b was set to 1250 cm/s [4]. Internal rear reflectance was modeled as perfectly diffuse, with R_b ranging in value from 0% to 100%. The results are shown in Figure 4.

Model calculations indicate that an efficiency improvement of 1.5% absolute is possible from the improved surface passivation of the metal/dielectric reflector over the metal reflector. For the metal reflector, efficiency swings 0.8% absolute over the full range of R_b; for the metal/dielectric reflector, it swings 1.5% absolute. The difference in the performance improvement at fixed R_b is attributed to the difference in surface passivation ($S_b = 10^6$ vs. 1250 cm/s). Notice that efficiency enhancement due to better back surface passivation increases with R_b, suggesting that improved surface coatings with lower S_b values, such as the oxide/nitride stack from [4], may enhance the effects of high R_b values.

Consider a cell with an ohmic contact and $R_b = 90\%$, corresponding to an Al contact fired at 700°C and an efficiency of 13.5%. Replacing this with an Ag metal/dielectric contact fired at the same temperature yields an R_b of ~ 98% and an efficiency of 15.7%. According to Figure 4, roughly a tenth (0.2%) of the improvement results from the improved BSR, with the remaining improvement (2.0%) resulting from enhanced surface passivation.

The Al paste, when fired at high temperature, can alloy with silicon and form a back surface field (BSF). Very low effective values of S_b have been reported from high-quality BSFs on single-crystal silicon [8]. The aforementioned PC1D model, using the S_b value of 1000 cm/s reported for $1\ \Omega \cdot$ cm silicon and, from Figure 3, $R_b = 82\%$ for the alloyed Al BSF, yields an efficiency of 15.5%. This is similar to the efficiency of 15.7% obtained using the screen-printed Ag metal/dielectric reflector. In contrast, a model corresponding to an evaporated Ag metal/dielectric BSR ($R_b = 97\%, R_{fi} = 20\%$, specular back surface) yields an efficiency of 14.9%. Thus, the screen-printed Ag metal/dielectric BSR developed in this study displays similar performance to a high-quality screen-printed Al BSF, and a distinct performance advantage over the evaporated Ag metal/dielectric BSR.

In addition to the 0.2% increase in cell performance, the metal/dielectric BSR has three other distinct advantages over the screen-printed Al BSF:

1. High-quality BSFs have been reported only by laboratory researchers; S_b values obtained by PV manufacturers for cofired full metal back commercial cells are typically higher than that used in the example above.

2. PV manufacturers *have* demonstrated that SiN_x layers can be used for large scale production and provide good surface passivation.

3. Full-back BSFs are known to create warping problems in thin substrates, which are the very substrates that would benefit most from a high-quality passivating back surface reflector.

Thus, the high-quality screen-printed metal/dielectric BSRs developed in this study are industrially-viable with current PV production technology.

4. CONCLUSIONS

Several screen-printed BSRs have been demonstrated. The back surface reflectance of screen-printed Ag reflectors on thin SiN_x dielectric layers has been shown to be similar to that of reflectors fabricated with evaporated metals. Furthermore, the effectiveness of these screen-printed reflectors is improved by high-temperature processing. Effective reflectors were also produced using an Al paste. However, they showed significant degradation at high processing temperatures. All of the screen-printed BSRs investigated in this study were highly diffuse, thereby enhancing the light trapping efficiency in planar silicon solar cells over that available from evaporated metal reflectors. Simulations using PC1D show that the performance of an Ag metal/dielectric reflector can exceed that of a high-quality Al BSF; furthermore, it can do so using processes that are well-established in the PV industry.

ACKNOWLEDGEMENTS

The authors wish to thank Todd Williams of the Ferro Corporation for supplying the Al conductor paste used in this work. This work was supported by U.S. Department of Energy subcontract XAF-8-17607-05 and National Renewable Energy Laboratory subcontract DE-FC36-00G010600.

REFERENCES

[1] M. A. Green, Silicon Solar Cells: Advanced Principles & Practice, University of New South Wales, Kensington, NSW (1992).

[2] A. Goetzberger, Proc. 15th IEEE Photovoltaic Specialists Conf. (1981) 867.

[3] F. L. Pedrotti, S.J., L. S. Pedrotti, Introduction to Optics, 2nd ed., Prentice Hall, Englewood Cliffs, NJ (1993).

[4] A. Rohatgi, P. Doshi, J. Moschner, T. Lauinger, A. G. Aberle, D. S. Ruby, IEEE Trans. Electron Devices **ED-47** (2000) 987.

[5] J. E. Cotter, J. Appl. Phys. **84** (1998) 618.

[6] J. M. Gee, Proc. 20th IEEE Photovoltaic Specialists Conf. (1988) 549.

[7] P. A. Iles, C. L. Chu, Proc. 25th IEEE Photovoltaic Specialists Conf. (1996) 109.

[8] S. Narasimha, A. Rohatgi, Proc. 26th IEEE Photovoltaic Specialists Conf. (1997) 63.